

## Appendix D

# Working Model for Reservoir Development

### Table of Contents

Introduction .....	2
Guiding Principles .....	3
Proposed Model .....	4
Supporting Concepts.....	7
Theoretical Versus Practical System Behavior .....	7
The Role of Temperature .....	10
Tectonic Influence .....	14
Uplift Model Validation.....	16
Recap and Summary.....	21

## Introduction

After twenty years of production operations in the tight gas reservoirs of the Rockies, producible (moveable) water is being encountered with increasing frequency. This represents a significant paradox with respect to historical assumptions of these deep geopressured basinal areas being relatively “dry” i.e., without significant moveable water. A better understanding of the nature and occurrence of the water problem is necessary to avoid producing unacceptably large quantities of unwanted water.

The conclusions of the water geochemistry portion of the project were assessed for impact on the practical aspects of the basin-centered gas hypothesis. As presented by various authors and modified by the authors’ experience, this assessment generated new key questions:

- 1) When there is little mass movement of water except in local areas of structural complexity, and traps form and gravity segregation occurs wherein the saturation of gas increases at the expense the native waters (2004 Shanley, et al), *by what mechanism does the gas force the native water out of the trap?*
- 2) If gas and fluid movement is restricted by relative permeability relationships, and assuming it could force the native water out (presumably flow-restricted for the same reasons), *how does the gas move in sufficient volumes to accumulate?*
- 3) While some fracture zones produce high rates of gas, *how and why do other fracture zones produce water at high rates?*

The key to avoiding or remediating unwanted water production during development operations seemed to lie in answering these questions. A conceptual reservoir development model was used as a vehicle to organize the diverse observations and satisfy the following guiding principles.

## Guiding Principles

Certain principles guided and governed the development of our working model for tight gas reservoir development. These principles were derived from our studies of gas-charged basins with producible formation water as well the previous work of others.

1. Produced water compositions generally reflect host rock environments of deposition. (2004 Henry and Billingsley).
2. Areas of faulting and vertical transport may be indicated by anomalous chemical and/or isotopic compositions as measured against background regional trends (2004 Henry and Billingsley).
3. One study of water chemistry suggests gas and water production from coals. (1998 Smith and Surdam).
4. Gravity segregation of some gas accumulations in the Greater Green River basin is well-documented (2004 Shanley, et al).
5. The impact of stress dependency on relative permeability is mathematically corroborated by Ostensen (1983), Byrnes (1997) and Shanley (2004).
6. The significant role of temperature in generation of subsurface stress as established by Warpinski (1989), Engelder (1985), and others.
7. The role of poro-elastic effects during uplift of gas charged sediments as documented by Katahara and Corrigan (2002).
8. Last, but not least we took into account that:
  - The ability of water to flow in the deep subsurface is more restricted than gas; water is more easily characterized chemically than gas.
  - Most significant large-scale tight gas basins have undergone significant uplift after gas generation.

Every effort was made to test and affirm the component ideas that comprise the overall model within both theoretical considerations and practical evidence. In discussing the model, a general overview will be followed by a review of supporting theoretical concepts, practical examples and a summary.

## Proposed Model

This is a general overview of the conceptual reservoir development model we advocate. The model concept was first presented as a “poster” at the American association of Petroleum Geologists (AAPG) Hedberg Conference on Tight Formation Gas in Vail, CO, April 2005, and then later that same year as an oral presentation to the Calgary AAPG Convention. For further reference these presentations can be viewed in full at [AAPG Calgary 2005 Concept.ppt](#), [AAPG Hedberg 2005 part-1.pdf](#) and [AAPG Hedberg 2005 part-2.pdf](#)

This project explored alternative avenues for the development of the large-scale unconventional gas accumulations termed “continuous” by the United States Geological Survey (USGS), and known to contain areas of higher productivity paradoxically exhibiting more conventional characteristics (water production, among others) as described by Shanley, et al (2004). Different routes to this endpoint would offer alternative strategies for successfully avoiding or remediating water in these tight gas accumulations. *Our model neither answers all questions nor resolves all the apparent conflicting aspects of basin-centered gas as a comprehensive tight gas reservoir development model exceeded the scope of this project.*

This conceptual model honors generally accepted principals of geology such as petrophysics, rock mechanics and reservoir engineering. It does differ from more typical reservoir development conceptualizations in several important aspects. While many of the supporting concepts incorporate assumptions of elastic material behavior, the overall reservoir development process itself is envisioned as essentially inelastic.

This inelastic process is a series of nonlinear, irreversible mechanical, and chemical transformations that occur in response to changing conditions of temperature and pressure. Generation of hydrocarbons from source rocks is an example of an inelastic process. Others are grain-crushing and pressure solution during mechanical and chemical diagenesis. Thermoelastic expansion and contraction of individual mineral grains or rock fragments solely in response to temperature changes is an elastic process. *In this model rock and reservoir properties are envisioned to inelastically change through time, in response to shifting pressure and temperature conditions.*

Fig. D-1 is a simplified graphical illustration of the reservoir development cycle. The cycle is divided into Phase I (generally burial) and Phase II (generally uplift). The transition between Phases I and II is placed at the time of maximum burial. There is probably some overlap in event timing. Gas generation may not end with the onset of uplift, or structural activity may initiate natural fracturing before maximum burial but, in general, the reservoir has lost most of it’s primary porosity, has extremely low permeability and neither gas nor fluid is mobile for production purposes. Shanley, et al (2004) described this general setting in detail.

## Key Development Stages of the Working Model

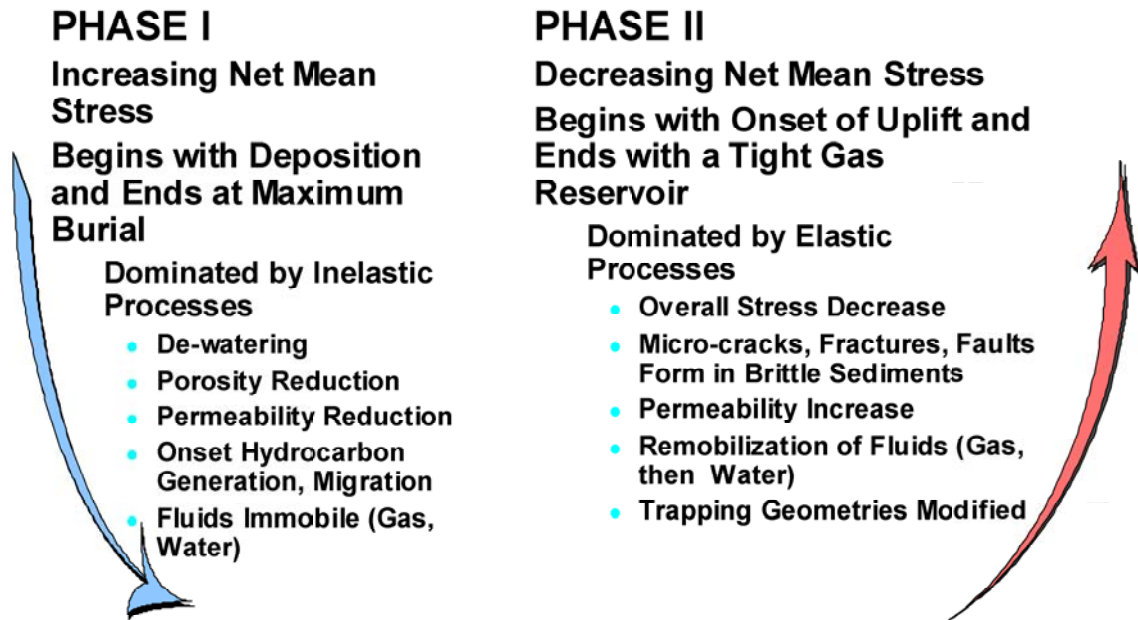


*Fig.D-1 Key Reservoir Development Stages*

Several simultaneous and potentially inter-related processes are active on the reservoir. Transformation of thermal and kinetic energies into chemical and physical alterations of the rock matrix occurs frequently. Kinetic energy may also be stored elastically in a compacted matrix, stabilized with diagenetic cements and released later when falling pressure/temperature conditions allow binding intergranular cements to fail. As a result, development of reservoir fabric elements such as natural fractures may be displaced in time or exhibit counter intuitive behavior. Warpinski (1989) discussed the implications of a lithology dependent stress relaxation component in his viscoelastic modeling efforts. Lajtai and Alison (1979) demonstrated counter-intuitive material behavior in practical laboratory experiments.

Pore and pore throat geometries change through time. Original intergranular permeability, both absolute and relative, is envisioned to be near zero at maximum burial depth (end of Phase I). Permeability (and minor porosity) is developed in new forms, with different pore geometries and behavior, during uplift (Phase II). Ostensen (1983) relates tabular pore throat geometries through mathematical analysis to tabular, slit-like grain-bounding micro fractures. The permeability regeneration process begins with microfracturing at grain scale and builds to the development of the regional natural fracture systems so common in the Rockies. A major kinetic energy source to drive the extensional fracturing process is supplied by the back transformation of accumulated thermal energy (through cooling) to strains internal to the reservoir (extensional natural fractures).

Horizontal stress is applied to the reservoir sediments asymmetrically by regional tectonic compression and shortening. Basement fault movement generates local shearing in the overlying sedimentary units. Strain energies, stored in the sediments during regional compression, are released during uplift (displaced in time) and influence the orientation and intensity of the regional natural fracture systems. Reservoir permeability to fluids and gases, lost in the burial phase (Phase I) is regenerated in an alternate form, by different mechanisms, during the uplift (Phase II).

Gas generation is envisioned to be isotropic in nature and contributes to fracturing energy during uplift but does not by itself cause fracturing during the burial phase. Fluids are present in the system throughout the process. The fluids are initially mobile, become immobile at maximum burial and, if pore throat apertures and relative permeability conditions are satisfied, may again become mobile during uplift.

These cycles of burial and uplift, energy input, transformation and release, control mechanical and chemical diagenesis of sediments through time. The general sequence of diagenetic events affecting porosity and permeability destruction in clastic sediments with increasing burial is well documented. There has been less focus on documenting diagenetic events during an uplift (energy release) phase. *The impact of stress reduction on reservoirs during uplift may be an important, underestimated mechanism for permeability enhancement of tight reservoirs.*

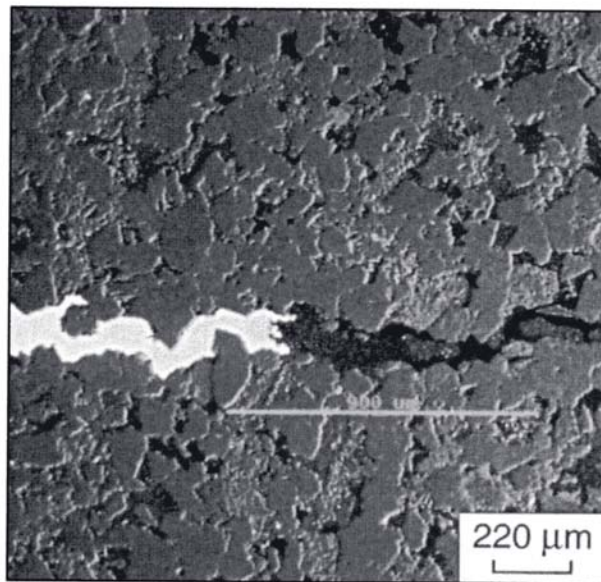
## Supporting Concepts

### ***Theoretical Versus Practical System Behavior***

Natural systems often exhibit differences between behavioral characteristics projected on the basis of theory and the practical results of experimentation. The classic geologic example of this phenomenon is the derivation of failure angles by Anderson (1951) where the theoretical shear failure angles are predicted to be 45 degrees from the principal horizontal stress and in practice form consistently at around 30 degrees.

A lesser-known example is the Griffith material concept developed in the early twentieth century. It documents the observed paradox between material strength calculated on the basis of molecular bonding forces and the observed practical strength of materials during laboratory testing. Griffith hypothesized the presence of microscopic cracks disseminated throughout the material to account for the differences between theoretical calculations of material strength and practical strength as established through actual failure.

Grain bounding microcracks, as modeled by Ostensen, would fulfill the same role, at a much larger scale, in a sandstone. This would account for the relatively rare crossing of grain boundaries by extensional fractures (as in fig. D-2). This general mechanism is proposed for the initiation of rock failure during uplift.

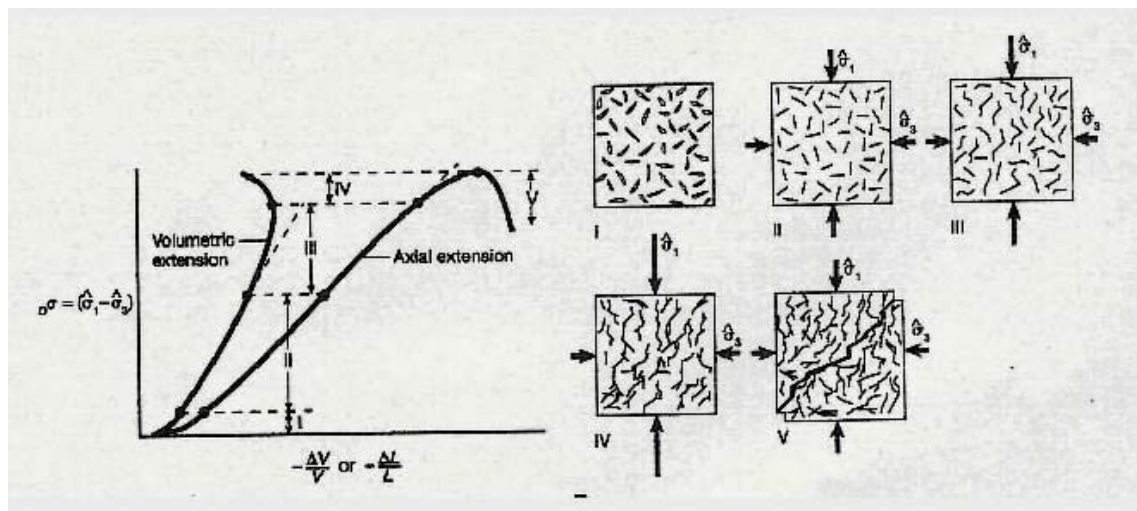


Backscatter scanning electronic microscope (SEM) image of an Almond natural fracture (Amoco Production Co., Champlin 254B-2, T20N, R93W). The fracture was originally oriented near vertical. The vertically trending textural change on the left is remnant bedding. The fracture forms as a coalescence of smaller fractures and for the most part avoids the major grains. Other faint planar segments are visible across the image. The bright fracture fill is barite

***Fig. D-2. Backscatter SEM of an Almond natural fracture***

Engelder and Fisher (1996) applied the broader Griffith energy balance concept to the problem of regional fracture development. They found that “fixed grips” boundary conditions were a reasonable approach for thermoelastic fracture problems (discussed later).

The Griffith concept, in fig. D-3 (1992 Twiss and Moores), illustrates effective resolution of an apparent paradox, as a practical vision of microcrack distribution between grains within a clastic rock as well as a reasonable mechanism for the development of regional extension fractures.



Griffith derived his material behavior concept in the early 20<sup>th</sup> century, to explain material failure at the molecular level. From a practical standpoint, however, the distribution of microcracks through a superficially homogenous medium seems like a very good conceptual tool to explain the material properties of reservoir rocks with grain bounding microfractures. Note the similarities in general appearance between the idealized representation in this figure (stage V) and the backscatter SEM of an Almond natural fracture (see fig. D-2).

**Fig. D-3. Griffith material concept**

Sedimentary rocks are generally defined as coeval aggregates of loose constituent grains deposited, and later compacted and cemented during burial in a subsiding geologic basin. The constituent grains can be either mono-mineralic or poly-mineralic in nature. The composition, size and degree of interstitial cementation of the grains are generally accepted to affect the material properties (porosity, permeability, strength, etc) of the sedimentary rock.

The relationships between the constituent grains can and do change through time as mechanical and chemical diagenesis proceeds with burial. Given the composite nature of sedimentary rocks, our assumption is that the grains themselves are very nearly the smallest mechanical units. Mathematically upscaling the composite system to calculate the expected mechanical behavior of the rock as a function of the component grains, porosity, pore fluids and pressure is the subject of numerous studies in poro-elastic behavior of materials (and beyond the scope of this report). A common theme of these studies is the significant impact of temperature changes on the sizes and shapes of constituent grains.

Mechanical and chemical changes occurring during burial act along the margins of the grains, at least initially. Grain-crushing will increase the number of boundaries and allow closer packing of the grains, reducing porosity and permeability, thus affecting the basic mechanical properties of the rock.

The dominant grain-scale failure mechanism of this process is shear as the grains are forced into and past each other. Grain-crushing during mechanical compaction occurs in an environment of increasing mean confining stress as the rock undergoes progressive compaction.

In contrast, extensional rock failure initiates and propagates along the zones of greatest mechanical weakness, most likely the grain boundaries. Failure by extension under a “fixed grips scenario” has the net effect of increasing the volume of the rock by the creation of void space along the zones of failure. Bourne (2001) used a modified Griffith-Coulomb failure criterion to demonstrate that it is extremely difficult to cause tensile failure in rocks during periods of increasing net mean stress. Tensile failure is most common during periods of falling net mean stress, mainly attributed to regional uplift and cooling by Bourne.

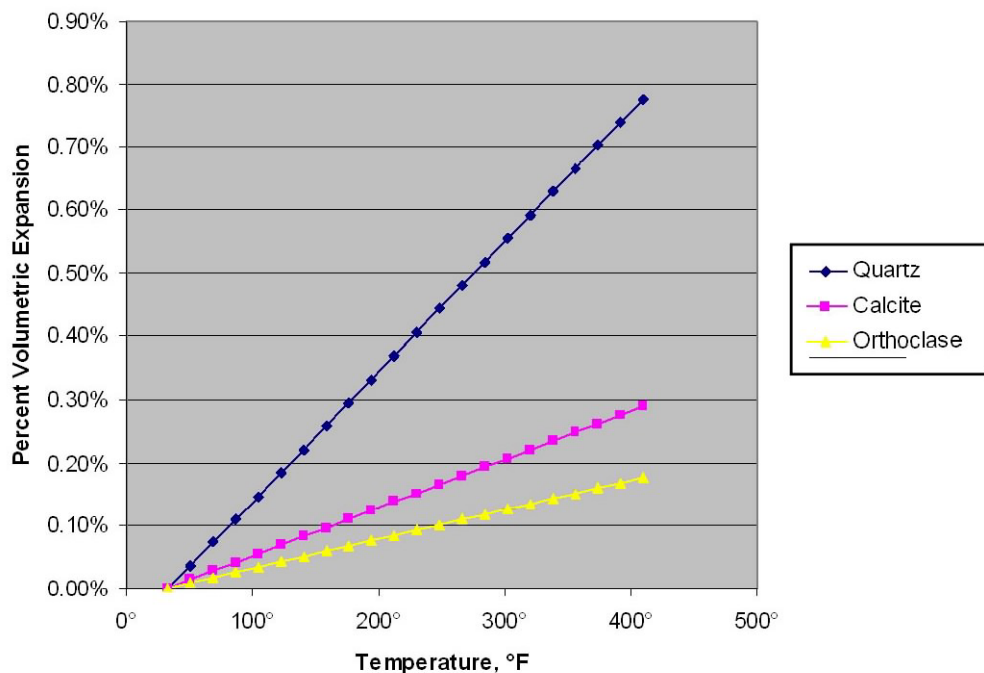
*Thus there is a fundamental difference in the processes active in rocks at the grain scale during periods of net confining stress increase and decrease.* The physical differences are visible at the grain scale through microscopic and laboratory techniques. This fundamental difference is the basis for the two-phase developmental process underlying the conceptual model set forth here.

## The Role of Temperature

Temperature cycles associated with burial and uplift of reservoir sediments are major factors responsible for developing reservoir permeability.

Published data show that quartz, a major constituent of sandstone reservoirs, is one of the more thermally sensitive minerals commonly found in clastic rocks. Calcite and orthoclase feldspar are also significantly sensitive to thermal changes. These materials expand and contract with cycles of temperature change during burial and uplift and can generate large intra-basinal stresses. Unless the basin margins are allowed to expand and contract in concert, temperature-driven volume changes of these materials, within the basin fill, generates large isotropic stresses, apart from and in addition to any lithostatic or tectonic stresses.

Warpinski (1989) noted significant impact of thermally generated stresses and associated strain in his viscoelastic simulations. In his Piceance Basin analysis, the strains generated by temperature effects were the same order of magnitude as tectonic strains. This phenomenon is graphically illustrated in fig. 4, which depicts the impact of heating on a perfect sphere of quartz (fig. D-4).



Thermo-elastic stress generated by grain expansion is a major (~40%) component of burial stress. Quartz is significantly more sensitive to temperature than other common constituents of the reservoirs.

**Fig. D-4. Thermo-elastic expansion of a spherical quartz grain**

The coefficient of thermal expansion (CTE, mm/m-°C) for quartz is well constrained because of its use in the semiconductor industry. It varies between optical axes with the a and b (equal) axes being approximately twice that of the c axis (~8 mm/m-°C). An initial hypothetical sphere of quartz becomes oblate, increasing its volume by nearly 0.8% when heated to 400 degrees Fahrenheit. Calcite, the next most thermally sensitive common reservoir component increases its volume only 0.3 % and orthoclase still less at 0.18 %.

These general relationships hold true when the minerals are included in composite systems (fig. D-5). Granite (with the most quartz as a constituent) has the highest coefficient of thermal expansion. The thermal behaviors of other types of igneous rocks also reflect their mineral compositions. On balance, the more quartz there is in a rock, the higher the coefficient of thermal expansion.

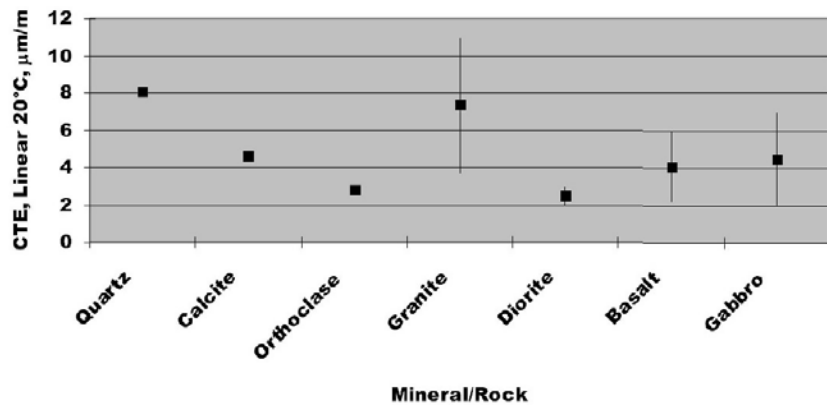
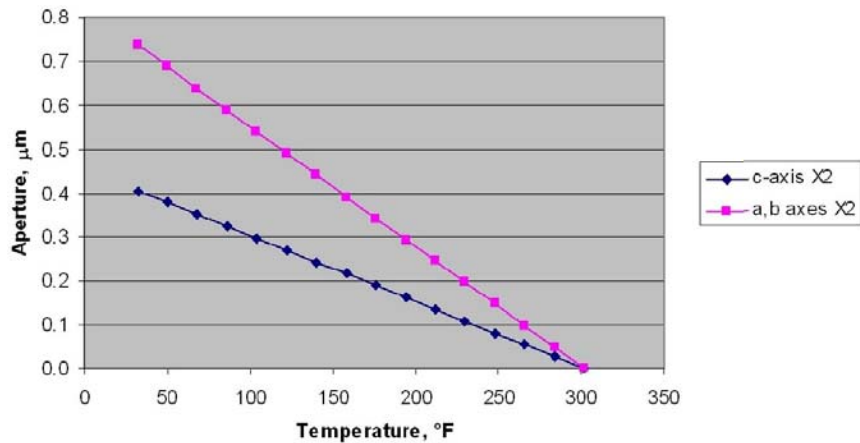


**Fig. D-5** Coefficients of thermal expansion of common constituents

Fig. D-6 illustrates the mechanism proposed for permeability generation by cooling of the matrix. Assuming roughly spherical (0.17 mm radius) quartz grains, packed tightly at 300 degrees Fahrenheit, the grains will shrink anisotropically along the crystallographic axes, proportionally, according to their respective coefficients of thermal expansion.

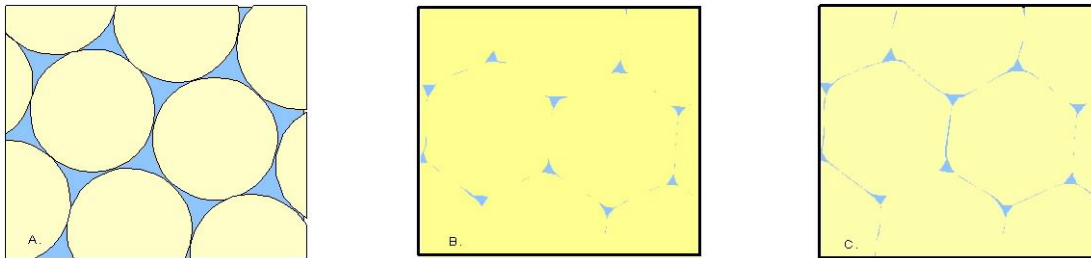


Maximum aperture between adjacent quartz grains cooled from 300 F° (.17 mm original radius)

**Fig. D-6.** Generation of permeability through cooling

If the grains are assumed to be stationary with respect to each other, an aperture will form with a width controlled by the relative relationships between the axes of the cooling grains. This is shown diagrammatically in fig. D-7. Ostensen (1983) used mathematical analysis of stress-dependent permeability behavior in tight-gas sand cores to postulate tabular pore geometries with comparable apertures.

Thermal expansion of the constituent grains generates internal stresses that contribute to the process. These diagrams (fig. D-7) illustrate this cycle (exaggerated for visibility).



A. Schematically depicts an original closest packing arrangement of the sand grains.

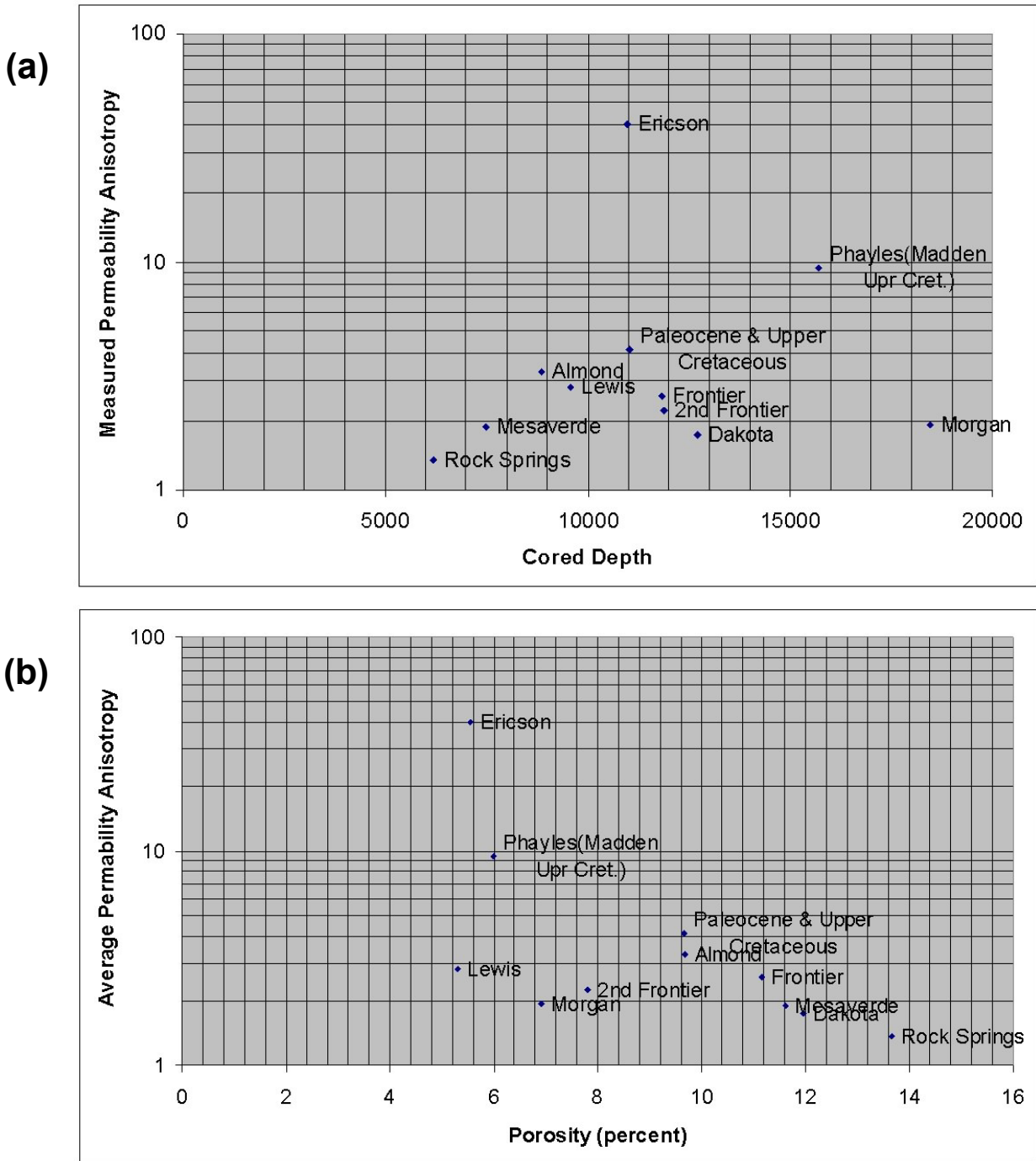
B. Depicts the sand at its maximum burial when most of the original porosity has been destroyed, the grains are in pressure solution contact, and the remaining porosity is isolated.

C. Illustrates a 0.04% decrease in grain radius from cooling during the uplift process. This would be the equivalent of being uplifted from 15,000 to 10,000 feet subsurface. Sediment composed of pure 0.00017 radius quartz grains would generate grain-bounding cracks between 0.2 and 0.4 microns disseminated throughout its matrix.

***Fig. D-7 Cycle of thermal expansion of constituent grains generates internal stresses***

The aperture range depends on orientation with respect to the crystallographic axes. These values for microcrack permeability in tight gas sandstones are comparable to those calculated by Ostensen (1983). During this project a large volume of existing, whole core, porosity, and permeability data was collected from the Green River basin files while searching for produced water analyses.

In many instances, permeability in the whole core had been measured in two directions. Most cores showed significant permeability anisotropy (two-fold or greater). Notably, core from the Ericson formation exhibited the greatest permeability anisotropy (figs. D-8a and D-8b).



Historical whole core, two direction, porosity and permeability data collected during this project shows that the greatest permeability anisotropy is observed in the Ericson, a quartz-rich member of the Mesaverde group. The Ericson has less porosity than other units, even though the other cores were recovered from greater depth. To the extent it reflects true conditions in the subsurface, this data also suggests a significant amount of permeability anisotropy may be present at the grain scale in the subsurface.

**Fig. D-8 a and b. Permeability impact of cooling and composition on permeability**

Such anisotropy has been traditionally attributed to lithostatic stress release associated with the coring process. Re-examination of this data, however, suggests mineral composition responding to cooling (during extraction to surface) may have a significant influence on the rock response. If the relative subsurface stress component associated with temperature predicted modeling is correct, then the composite coefficient of thermal expansion (determined by rock mineral composition) becomes a major permeability control.

### ***Tectonic Influence***

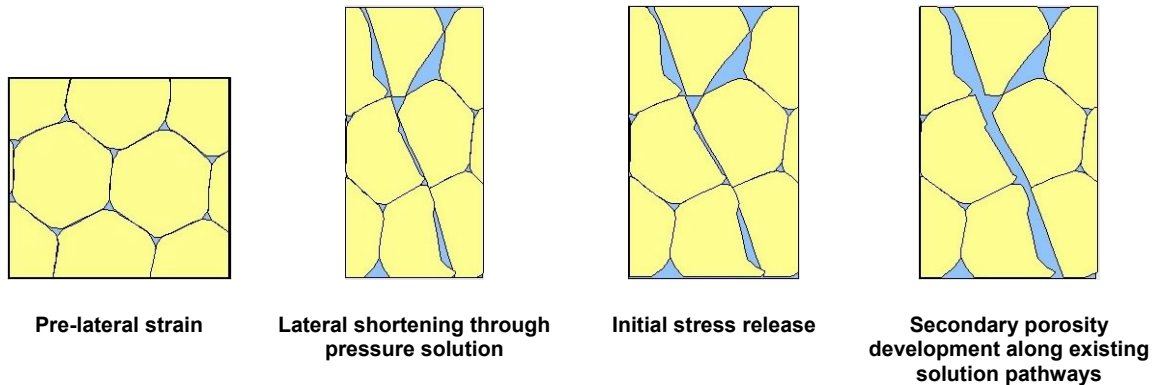
Regional tectonics plays a multi-faceted role in the development of tight gas reservoirs. In addition to profoundly affecting the basin development, subsidence, stratigraphy, and structure, it also can have a diagenetic impact on the sediments. Warpinski (1989) estimated the lateral strains in the multi-well experiment (MWX) area of the Piceance to be approximately the same magnitude as the thermoelastic fraction.

If burial stresses crush grains and promote pressure solution it is likely basin scale tectonic stresses will have a similar impact. Significant differential lateral stress will preferentially compress the sediments, imparting a weak fabric of planar compressional strain features such as pressure solution boundaries and vertical stylolites. *Generally these planes will be oriented perpendicular to the principal horizontal stress and reach maximum development in areas of the greatest shortening strain.*

Laboratory experiments (1979 Lajtai and Allison) have shown that wet mortar—stressed, allowed to solidify, and released—will fracture perpendicular to the applied principal horizontal stress and even generate some load parallel fracture sets to accommodate the extension. Present day maximum principal horizontal stress is commonly oriented perpendicular to the inferred (from macro structural relationships) paleo principal horizontal stress.

To illustrate such a relationship in the Pinedale anticline area, borehole image interpretations were presently separately by BP and Ultra to the Wyoming Oil and Gas Conservation Commission (WOGCC). This phenomenon would yield coplanar compressional and extensional features potentially creating confusion when unraveling local structural history.

Fig. D-9 diagrammatically illustrates a potential tectonic relaxation fabric with secondary porosity generation. Planar features with secondary porosity development, as illustrated by Webb, et al (2004), are relatively common in Rocky Mountain tight gas sands areas. Fluids under-saturated in calcite, moving through such a pore system, could very likely be responsible for leaching cements or unstable components.



These diagrams schematically illustrate the potential for development of pressure solution surfaces along grain-to-grain contacts that may then relax and dilate after active compression and/or uplift. Circulation of undersaturated fluids along these pathways has great potential to foster development of secondary porosity on uplift. (Detailed in Appendix C.)

**Fig. D-9. Strain and pressure solution**

## ***Uplift Model Validation***

This uplift model for permeability development was validated using two data sets acquired by independent groups, published fifteen years apart. Keighin, et al (1989) published the results of an extensive petrology and reservoir property study on the Almond formation of the GGRB. The study contained detailed petrography, core analysis, and vitrinite reflectance (Vr) results, from twenty-five Almond cores.

Roberts, et al (2004) published a detailed assessment of oil and gas generation timing covering the general United States Geological Survey (USGS) southwestern Wyoming assessment area. These two data sets are interpreted and integrated to show uplift as a significant influence on permeability.

Keighin, et al, collected petrographic, petrologic, core analysis, and maturity data on Almond cores from across southern Wyoming during resource assessment activities. Twenty-five cores were studied. Core analysis data ( $\phi$ , k) was presented on twenty-three cores (Table D-1).

Twenty-two contained usable, paired core analysis and maturity data values (four of the twenty-two used were noted to have had projected %Ro values). Their findings underscore a recognizable but poorly understood relationship between core analysis properties and organic maturity (as indicated by Vr).

**Table D-1. Porosity, permeability, & Vr data from cores in Almond Fm, SW Wyoming**

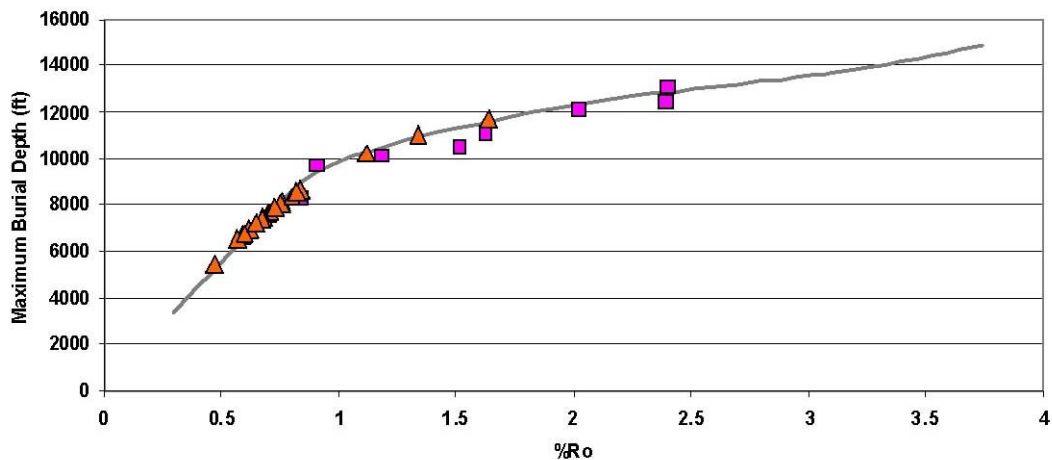
Well No.	Well Name	Location	Core Interval (ft)	Porosity (range & average %)	Permeability (range & average md)	Ro %	Norm_k	Proj Max Burial Depth	Amt of Uplift
1	Colo Interst Gas 2-8-14-92 Blue Gap 11	SW ¼ SW ¼ Sec 8 T. 14 N, R. 92 W	9,059 – 9,091	1.7 – 10.0 (5.0)	0.01– 5.9 (0.75)	0.80	0.15	11,598	2,523
2	Pan Am Barrel Springs 3	NE ¼ NE ¼ Sec 11 T 16 N, R 93 W	8,407 – 8,441	7.4 – 16.1 (12.0)	0.01– 0.30 (0.07)	0.70	0.0058	10,838	2,418
3	Amoco 1 Champlin 535 Amoco A	C SW ¼ Sec 17 T 16 N, R 97 W	13,645 – 13,674	2.4 – 11.5 (8.0)	0.02– 1.7 (0.34)	1.64	0.0425	14,951	1,301
4	Amoco Champlin 336 Amoco A-1	NEI ¼ SW ¼ Sec 21 T 17 N, R 94 W	10,626 – 10,649	2.6 – 12.0 (5.9)	0.01– 0.65 (0.08)	1.12 P	0.0135	13,405	2,770
5	Champlin Higgins 13A	NW ¼ NE ¼ Sec 7 T 17 N, R 98 W	6,992 – 7,013	8.2 – 17.1 (13.8)	0.02– 1.9 (0.48)	0.59	0.0347	9,873	2,873
6	Amoco 1 Champlin 440 Amoco A	NW ¼ NW ¼ Sec 11 T 17 N, R 98 W	8,590 – 8,638	1.5 – 6.2 (3.9)	<0.01– 4.9 (0.35)	0.84	0.8974	11,873	3,253
7	Amoco 1 Champlin 534	C SW ¼ Sec 31 T 18 N, R 96 W	10,969 – 10,990	3.9 – 11.0 (7.8)	0.02– 0.1 (0.07)	0.76	0.0089	11,307	327
8	Champlin Federal 44-4	SE ¼ SE ¼ Sec 4 T 18 N, R 98 W	6,841 – 6,897	2.3 – 19.2 (12.4)	0.03– 24.0 (2.40)	0.75	0.1935	11,232	4,372
9	Champlin UPRR 44-9-2	SE ¼ SE ¼ Sec 9 T 18 N, R 98 W	6,780 – 6,836	10.5 – 17.5 (14.6)	0.24– 6.06 (1.83)	0.71	0.1253	10,919	4,119
10	Texaco Table Rock 68	NE ¼ SW ¼ Sec 19 T 19 N, R 97 W	6,577 – 6,731	0.8 – 17.7 (8.1)	<0.01– 2.39 (0.33)	0.73	0.4074	11,078	4,438
11	Marathon 1-23 Tierney II	C SW ¼ Sec 23 T 19 N, R 94 W	N.A.	N.A.	N.A.	N.A.	N.A.	N.A.	N.A.
12	Forest 9-G-1	SW ¼ NE ¼ Sec 9 T 19 N, R 98 W	5,754 – 5,770	14.0 – 21.4 (17.7)	0.23– 41.0 (12.02)	0.62	0.6790	10,151	4,391
13	Forest 3-19-2 Arch	SW ¼ SW ¼ Sec 19 T 19 N, R 98 W	N.A.	N.A.	N.A.	N.A.	N.A.	N.A.	N.A.
14	Forest 1-8 Arch 70	SE ¼ NE ¼ Sec 1 T 19 N, R 99 W	4,794 – 4,812	11.5 – 23.9 (19.8)	3.1– 102.0 (23.57)	0.68 P	1.1904	10,673	5,873
15	Forest 63-2-2 Arch	SE ¼ SE ¼ Sec 2 T 19 N, R 99 W	4,485 – 4,527	14.9 – 23.2 (19.5)	1.5– 88.0 (31.0)	0.67	1.5897	10,589	6,089
16	Forest 20-23-4 Arch	SW ¼ NE ¼ Sec 21 T 19 N, R 99 W	4,497 – 4,528	18.8 – 25.6 (22.1)	0.21– 135.0 (43.96)	0.57 P	1.9891	9,682	5,172
17	Amoco Champlin 441 Amoco A	C SE ¼ Sec 21 T 20 N, R 95 W	9,142 – 9,178	0.9 – 5.7 (3.5)	0.01– 0.09 (0.03)	0.80	0.0085	11,598	2,438
18	Forest Mustang 1-22-1	NE ¼ SE ¼ Sec 22 T 20 N, R 97 W	7,452 – 7,513	12.3 – 18.9 (16.1)	<0.01– 0.9 (0.4)	0.60	0.0248	9,967	2,477
19	Luff 1-23 Champlin-Playa	SE ¼ SE ¼ Sec 23 T 20 N, R 99 W	4,577 – 4,600	7.6 – 16.7 (13.0)	0.08– 13.0 (2.94)	0.60	0.2261	9,967	5,377
20	Luff 4-29 Champlin	NW ¼ SE ¼ Sec 29 T 20 N, R 99 W	3,474 – 3,481	14.7 – 19.6 (17.3)	0.43– 18.0 (7.9)	0.47 P	0.4566	8,648	5,170
21	Amoco Champlin 527 Amoco A-1	C SW ¼ Sec 19 T 21 N, R 95 W	8,971 – 9,061	2.3 – 15.2 (10.7)	0.01– 0.93 (0.20)	0.65	0.0186	10,417	1,402
22	Amoco 1 Champlin 446 Amoco A	NE ¼ SW ¼ Sec 15 T 22 N, R 90 W	14,256 – 14,271	1.0 – 8.1 (4.5)	0.01– 0.14 (0.07)	1.34	0.0155	14,219	-45
23	Amoco 438 Amoco A	C SE ¼ Sec 5 T 22 N, R 96 W	9,910 – 9,931	3.6 – 7.9 (5.1)	0.08– 0.22 (0.11)	0.82	0.0215	11,738	1,818
24	Mich-Wisc Red Dessert 1-33	NW ¼ SE ¼ Sec 33 T 24 N, R 94 W	12,515 – 12,586	3.4 – 9.1 (6.5)	<0.01 (<0.01)	1.64 P	N.A.	N.A.	N.A.
25	Energy Reserves 2-24 Nickey	NW ¼ SE ¼ Sec 24 T 24 N, R 96 W	11,884 – 11,916	1.8 – 7.6 (5.3)	<0.01– 1.8 (0.18)	1.60	0.0339	14,872	2,972

P = projected vitrinite reflectance  
N.A. = Not available

Roberts, et al (2004), interpreted the timing of petroleum generation in southwestern Wyoming as part of an overall petroleum system assessment. Burial histories and seven synthetic Vr curves were constructed and calibrated to recorded Vr values. A burial history curve defines the relationship between depth of burial (used to calculate temperature), time (related to stratigraphy), and Vr. Vitrinite reflectance acts as a proxy for depth in areas where the relationship was calibrated. Because Vr continuously increases with maturity (depth), it reflects the maximum depth of burial. The Adobe Town (south central Washakie Basin) calibration is used as the standard Vr-depth relationship for purposes of our study.

A maximum depth of burial was calculated for each of the Keighin study Vr samples. This was done by digitizing the continuous (estimated) Vr curve published by Roberts, et al (2004), to generate a fourth-degree polynomial fit. The resulting equation was used to calculate a maximum depth of burial for the core Vr values.

Fig. D-10 shows the original calculated Vr curve (2004 Roberts, et al), the original calibration points (squares), and the calculated depths of burial for the Almond Vr samples (triangles). The final maximum burial depth values calculated were adjusted by a linear shift of 3,200 feet to account for recent uplift and erosion in the Adobe Town area (2004 Roberts, et al).



This graph illustrates the excellent fit between the

- Adobe Town easy %Ro model—*grey line*—(Roberts, et al)
- Original burial history calibration points—*squares*—(Roberts et al)
- Back projected maximum burial depths for the I petrographic/Vr data set—*triangles*—(Keighin, et al)

**Fig. D-10. Vr (% Ro) maximum burial depth calibration**

An estimated amount of uplift was calculated for each core location by subtracting the core depth from the estimated maximum burial depth. The Adobe Town area is very near the deepest portion of the present-day eastern GGRB. The resulting amounts of uplift were positive with only one exception, which calculated at fifty feet (for all practical purposes, 0). Thus the different vintages of Vr data are comparable; the burial history calculations and synthetic Vr profiles are reasonable; and the overall scheme used here to estimate the amount of uplift is judged valid.

Permeability (k) was normalized to porosity (phi) in order to correlate the reported permeability values (of Keighin) between cores. The data was reported as mean values of each attribute for each core. Mean permeability was divided by mean porosity to obtain a normalized permeability value for each core in terms of millidarcies per porosity unit. Keighin noted increasing degrees of scatter in the cores of lower porosity. This is most likely due to the permeability anisotropy observed in whole core analyses (as previously discussed).

A cross-plot of estimated uplift versus normalized permeability is shown in fig. D-11. The x-axis is the estimated uplift in feet vs. the normalized k on the y-axis in millidarcies/porosity unit (md/PU). The data show a strong positive correlation between increasing uplift, as projected from Vr differences, and normalized permeability from the core studies.

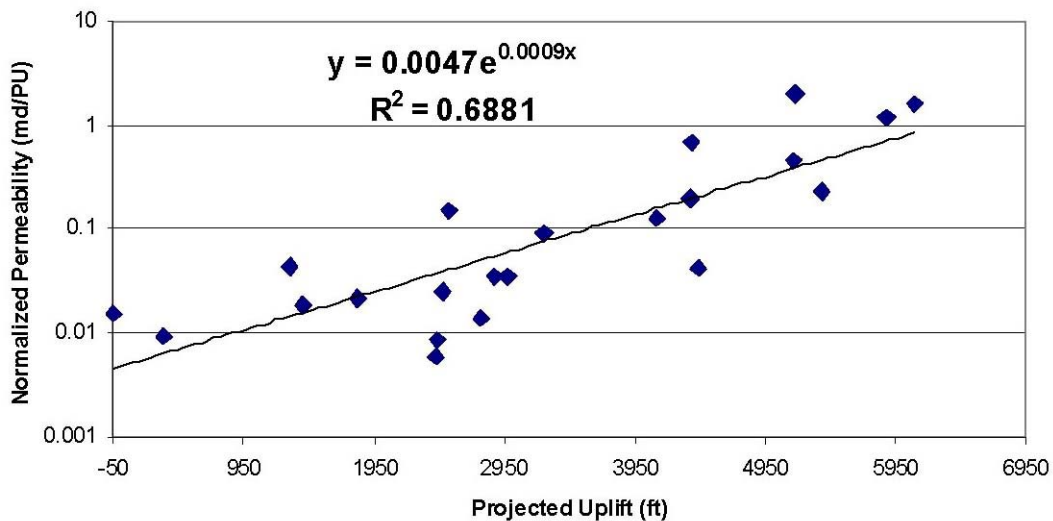


**Fig D-11. Projected uplift vs. normalized permeability**

There is some scatter to the relationship but the variance remains similar in magnitude across the range of uplift values. This scatter is due in part to the permeability anisotropy observed in whole core analyses noted previously. But it may also reflect differences in structural setting at the individual wellsites.

This analysis confirms a relationship between core analysis results and  $V_r$  first observed by Keighin, et al. However, the relationship is indirect and thus is defined by both maximum depth of burial *and* amount of later uplift. Rocks buried at shallow depths retain more of their original textures and gain little permeability upon uplift.

Rocks buried deeply lose the majority of their original permeability (permeability jail) and only regain permeability during uplift. Favorable quartz and calcite-rich facies improve more on uplift than quartz and calcite-poor facies, but there is little intrinsic value to either in the absence of uplift. In the absence of uplift or other stress release mechanisms, these rocks will remain relatively impermeable.

## ***Recap and Summary***

We advocate a schematic tight gas reservoir development model that is grounded in field observation, theory, and laboratory analyses. This model provides a mechanism for re-generation of intergranular permeability in sediments during uplift—after its complete or near-complete destruction during burial diagenesis.

Reservoir development is envisioned as a systematic process that occurs in two phases. The phases are differentiated on the basis of net mean stress *increase* (Phase I) and *decrease* (Phase II). Phase I processes destroy the majority of the primary inter granular pore throat geometries of the original sediment by compaction, grain-crushing, pressure solution and other, generally volume-reducing mechanisms.

During Phase II, net mean stress decreases and generates a different set of intergranular pore throats by a set of wholly different processes. The result is a reservoir with markedly different porosity/permeability characteristics than the original host rock.

The systematic effects of Phase I burial processes on sediments include a loss of porosity through diagenesis (mechanical and chemical), as well as generation, migration or adsorption of hydrocarbons. Mechanical compaction, de-watering, grain-crushing, pressure solution, chemical diagenesis, and gas generation are all viewed as sequential, irreversible responses to the higher temperature and stress associated with increased burial. The outcome for most rocks is a condition known as “permeability jail” (2004 Shanley, et al) where low porosity, low permeability and high water saturation leave little effective permeability for gas and water to flow. Gas-charged sediments remain in permeability jail unless tectonic activity begins an uplift process.

Phase II of the reservoir development process commences with the initiation of net mean stress reduction. Typically this is triggered by the onset of uplift, but gas generation and overpressure can impact net mean stress and usually precede maximum burial depth. Brittle failure with extension fracturing is another indicator of Phase II development.

Phase II processes may be wholly or partially elastic in nature in that a reversal (increase) in stress could theoretically close micropores and fractures. In practice, however, immediate diagenetic activity, such as precipitation of fracture propping fills, renders the overall process irreversible.

During Phase II, basin (or local) uplift systematically increases porosity and permeability. This eventually mobilizes gas and water (assuming the end-product is a gravity-segregated gas reservoir). Net confining stress decreases during uplift as a result of temperature reduction and unroofing.

Reservoir sands, particularly those high in quartz content, show a small increase in porosity as individual grains shrink and generate tabular, grain bounding micro-fractures (“tabular pores” –Ostensen and others). Gas, both as free gas in pores and sorbed gas in coals and organic shales, expands to fill the voids. It eventually establishes sufficient volume to migrate, either by diffusion or flow, leaving any remaining water in place.

As the uplift process continues, shrinkage of matrix grains reduces net confining stress and increases permeability. Fractures form as rock failure by extension is induced. The onset of macro fracturing increases total permeability within the reservoir and further facilitates gravity segregation.

Interbedded or overlying ductile shales have short stress relaxation times (1989 Warpinski); remain intact; and function as lateral or vertical permeability barriers. With sufficient stress release, the brittle reservoir may develop a large-aperture, saturated rectilinear-regional fracture system and behave as a dual permeability system. Interbedded coals and organic-rich shales may also store hydrocarbons and eventually release gas as reservoir pressures decline. *The uplift process; therefore, improves permeability for tight gas reservoirs.*

Large-scale uplift events are typically associated with faulting of the basement. Late-stage basement faulting propagates upwards through the sedimentary section, disrupts lateral continuity of sediments with varying scales of shear fractures, and further induces gravity segregation. These fault-related shear fracture systems can create areas of high permeability. If coincident with high gas saturation, they produce gas at high rates. Likewise, if coincident with areas of high water saturation, they (unfortunately) produce large volumes of water. If local saturation conditions for flow are met, open natural fractures of any type or size will move water.

This notion of general reservoir development includes a systematic increase of reservoir permeability by intergranular fracturing during uplift (or laterally by compression and relaxation) of a gas-charged sedimentary basin. This systematic process generates intermediate conditions favorable to gravity segregation of hydrocarbons and water. The final stages of the process can include development of extensive macro fracture networks and secondary porosity within the reservoir.